Multiscale Model For Pedestrian and Infection Dynamics During Air Travel

Sirish Namilae[1*], Pierrot Derjany[1], Anuj Mubayi[2], Mathew Scotch[3,4], and Ashok Srinivasan[5]

[1]Aerospace Engineering, Embry-Riddle Aeronautical University, Daytona Beach, FL, USA,

[2] S.A.L Mathematical Computational and Modeling Science Center, School of Human Evolution and Social Change, Arizona State University, Tempe, AZ

[3]Department of Biomedical Informatics, Arizona State University, Scottsdale, AZ, USA

[4]Biodesign Center for Environmental Security, Arizona State University, Tempe, AZ. USA

[5] Department of Computer Science, Florida State University, Tallahassee, FL, USA

Abstract

In this paper, we developed a novel multiscale model combining social-force based pedestrian movement with a population level stochastic infection transmission dynamics framework. The model is then applied to study the infection transmission within airplanes and the transmission of Ebola virus through casual contacts. Drastic limitations on air-travel during epidemics, such as during the 2014 Ebola outbreak in West Africa, carry considerable economic and human costs. We use the computational model to evaluate the effects of passenger movement within airplanes and air-travel policies on the geospatial spread of infectious diseases. We found that boarding policy by an airline is more critical for infection propagation compared to deplaning policy. Enplaning in two sections resulted in fewer infections than the currently followed strategy with multiple zones. In addition, we found that small commercial airplanes are better than larger ones at reducing number of new infections in a flight. Aggregated results indicate that passenger movement strategies and airplane size predicted through these network models can have significant impact on an event like 2014 Ebola epidemic. The methodology developed here is generic and can be readily modified to incorporate impact from outbreak of other directly transmitted infectious diseases.

Keywords: Infection Modeling, Pedestrian Movement, Air-Travel

---

[*] Corresponding Author – Email: namilaes@erau.edu

I. INTRODUCTION

Commercial air travel enables rapid transmission of infectious diseases across the globe. Travelers are in close proximity to each other and are susceptible to infection spread in common spaces such as airport boarding areas, lounges, security lines and within commercial airplanes. In addition, air travel brings together people from different geographic regions with different levels of vulnerability and receptivity due to variations in immunity, ethnic background, and intervention usage across geographic areas [1]. There is direct evidence for spread of infection within commercial airplanes for many infectious diseases including influenza [2], SARS [3], tuberculosis [4], measles [5] and norovirus [6].

Several factors affect the infection transmission in the high occupancy enclosed environment of aircraft cabins, including cabin air quality, exposure time, flight duration, and passenger contact due to inflight movement. The high efficiency particulate filters used in current airplanes are effective in reducing a contagion in the recirculated air [7]; however, virus shedding from infected passengers before the air can pass through filters can lead to other passengers becoming infected. In this context, passenger location and movement resulting in close contact between infective and susceptible populations is a critical component in infection spread aboard airplanes. Passengers move during boarding (ingress), deplaning (egress) and within the cabin. Susceptible passengers otherwise not exposed to the contagion may come into contact with it when they are in close proximity of infected passengers or contaminated surfaces during the high mobility phases of passenger entry and exit. There is a strong correlation between contact rates and infection rates in a number of disease epidemics including SARS [8] and Ebola [9]. The probability of infectious disease transmission when the host and agent come into contact is inherently stochastic and depends on variations in multiple factors including infectivity (virus content in bodily fluids and rate of shedding), age, and demographic characteristics. Stochastic infection models such as Susceptible-Exposed-Infectious (SEI) model have been effectively used in studying such infectious disease spread [10]. In this paper, we develop a novel hybrid model that combines a social force based pedestrian dynamical model with a stochastic infection transmission framework to study the effect of pedestrian dynamics on the infection spread.

Often there are limitations in modeling quantities related to real systems. Therefore, stochasticity is naturally inherent in systems, that is, there is uncertainty in its constituents. In order to address distinct types of uncertainty present in the system, we use scenario analyses into the aforementioned stochastic/probabilistic process based on SEI framework to allow for variance in projections of output parameters. We quantify the uncertainty in the input parameters as well as structural uncertainty in the model itself by simulating over the design space.

As a case study, we utilize the model to assess the propagation of Ebola aboard an airplane. Detailed pedestrian dynamics model enables tracking the trajectories of passengers that is needed to assess passenger contact rates due to different air-travel policies. During the 2014-15 Ebola epidemic, despite travel restrictions, there have been a few instances of Ebola infected travelers using commercial airplanes in the USA and Nigeria [11-13]. Models have suggested that 7.17 infected travelers per month would have been transported through commercial airlines without air travel restrictions [14]. Through the modeling framework developed in this paper, we assess the air-travel and passenger movement strategies that can reduce the infectious disease spread. The model developed here is general and can be potentially applied to additional airborne infectious diseases and extended to other crowded locations like airports.
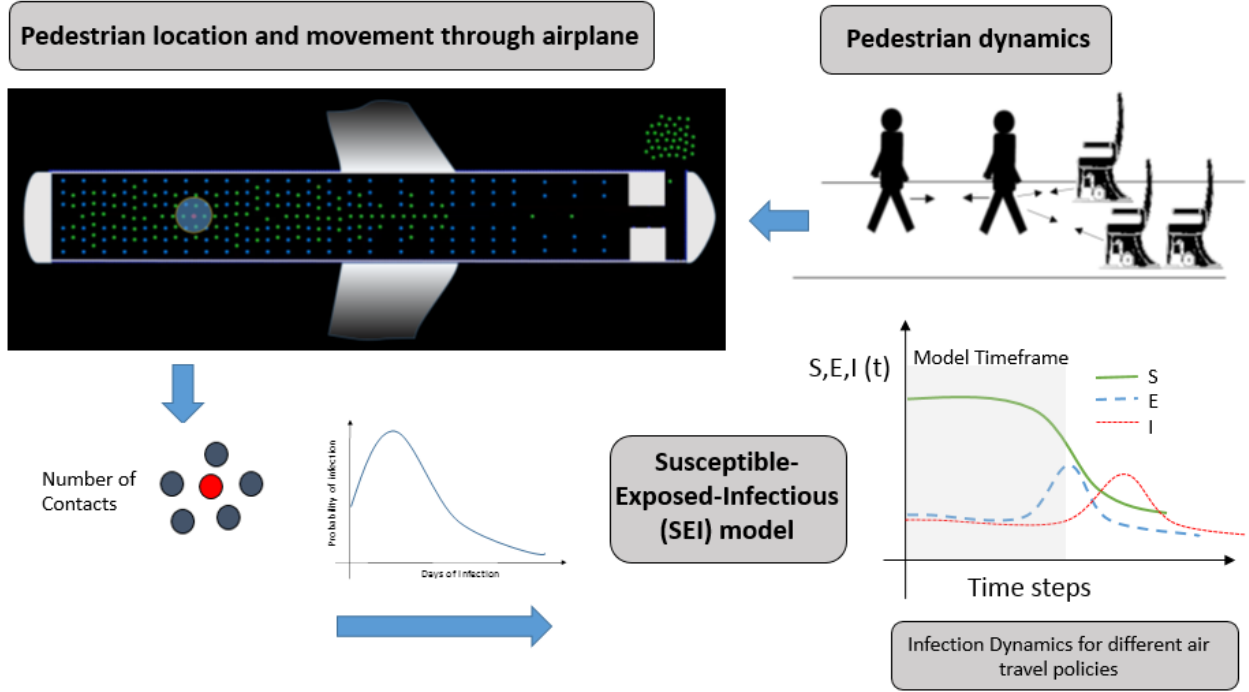
FIG. 1. Schematic depiction of the overall modeling approach

II. MODEL FORMULATION

We model the motion of pedestrians using a molecular dynamics based social force model [15]. Considering a pedestrian as a particle in motion, the pedestrian particle is subjected to competing forces of a person's desire to travel to a destination while impeded by obstructions (*e.g.* walls, chairs and other pedestrians). The total force experienced by a pedestrian:

$$\overline{F_i} = \sum \overline{f_i} = \overline{f_i^{int}} + \overline{f_i^{ped}} = m_i \overline{a_i} \tag{1}$$

Where $\overline{F_i}$ is the resulting force, $\overline{f_i^{int}}$ is the force exerted by the pedestrian in the intention to reach his/her terminus, $\overline{f_i^{ped}}$ is the resisting forces obstructing the motion, m_i the body mass and, $\overline{v_i}$ and $\overline{a_i}$ are the instantaneous velocity and acceleration at time t respectively.

The intention force relates the desired velocity of pedestrian i moving towards a destination $(\overline{v}_{0i})$ to the actual speed v_i and is defined by:

$$\overline{f_i^{int}} = \frac{m_i}{\tau} [\, \overline{v_{0i}}(t) - \overline{v_i}(t) \,] \tag{2}$$

Here, τ is a time step. We modify the equations of motion by introducing a local neighbor dependence to the desired velocity $\overline{v}_o^i(t)$. In line forming applications like in an airplane entry or exit, the self-propelling intention force and desired velocity of ith pedestrian is dependent on the position of nearest pedestrian in the direction of motion, i.e. in front of the pedestrian particle in the line. To model the slowing of pedestrian particle as they approach other particles in a line, the desired velocity of ith pedestrian $\overline{v}_o^i(t)$ in direction $\hat{e}_1$ is modified as follows:

$$\overline{v_{0i}}.e_1 = \left(v_A + \gamma v_B\right)\left(1 - \frac{\delta}{\overline{r_i}e_1 - \overline{r_i}e_1}\right) \tag{3}$$

In equation (3), $\widehat{e}_1$ is the direction of desired motion. For example, for passenger boarding an airplane, this could be the direction along the aisle. $(v_A + \gamma_i v_B)$ provides a distribution of desired speed for all pedestrians in the system. v_A is the deterministic component of the pedestrian speed. γ_i is a random number and $\gamma_i v_B$ is the component of pedestrian speed that varies for each pedestrian, enabling a distribution of speeds that accounts for differences due to factors such as age and sex. $\overline{r_i}$ and $\overline{r_k}$ denote the positions of ith and k^{th} pedestrians, where k^{th} pedestrian is the nearest in $\widehat{e}_1$ direction and $\left(\overline{r_i}\widehat{e}_1 - \overline{r_k}\widehat{e}_1\right)$ would be the separation between them in direction $\widehat{e}_1$. δ is the critical distance between two pedestrians in a line at which the rear pedestrian becomes stationary. Equation (3) ensures that attractive force toward destination is reduced when a pedestrian encounters another particle and the desired speed reduces to zero when the distance between them is δ.

The second part of particle dynamics in equation (1) considers the repulsive social force term $(\overline{f_i^{ped}})$ that inhibits the motion of pedestrian particles. The repulsive force is essential to ensure impenetrability of particles. For this purpose, we use the repulsive term [16] of Lennard-Jones potential given by:

$$\overline{f_i^{ped}} = \sum \overline{f_{iJ}} = \sum_{i \neq j} \nabla\varphi(\overline{r_{iJ}}) = \sum_{i \neq j} \nabla[\epsilon \left(\frac{\sigma}{r_{ij}}\right)^{12}] \tag{4}$$

where ϵ and σ are constants and r_{ij} is the distance between the ith and j^{th} pedestrians. The equation of motion in (1) is numerically integrated to obtain the velocities and positions in the subsequent time steps. We apply this approach to pedestrian movement in airplanes to obtain the trajectories of pedestrian movement for different boarding and deplaning methods. Note that equations (1-4) are in two dimensional space in the plane of pedestrian movement.

There are several parameters in the pedestrian dynamics model, such as maximum walking speed $(v_A + v_B)$, random variation (γ_i), distance parameter (δ), two parameters for the Lennard-Jones repulsive force terms (ϵ and σ) and aisle delay for luggage. There is experimental data available for some of the parameters like the range of walking speed [17, 18]. Also the observed exit times and passenger flow rate for some commercial airplanes is available in the literature [19, 20]. To obtain the estimates of other model parameters that represent realistic model behavior of an outbreak we vary the parameters over a large design space. In our earlier study [21], we used a parameter sweep on 60,000 processors to determine the parameters that match the available observed data of deplaning [19, 20]. We have been able to match the pedestrian dynamics model with experimental data on flowrates and exit times for five different airplane seating configurations for which test data is available. In addition, we have also been able to capture qualitative features like front to back unloading and hallway congestion [21]. The pedestrian dynamics parameters obtained through our earlier work [21] are used in the model and are tabulated in Table I.

The pedestrian trajectory information from the above model (equations 1-4) is integrated with a discrete-time stochastic Susceptible-Exposed-Infectious (SEI) model for infection transmission described below (equations 5-6). Note that in the context of air-travel of a few hours newly exposed (and infected) passengers do not become infectious. The schematic in figure 1 depicts the overall approach of this modeling study.

From a population of N passengers if i_c^0 represents number of infectives at a given time with age of infection of c, then the number of susceptible individuals at time t, S(t), is given by

$$S(t) = N - \sum_{c=1}^{d} i_c^0 = N - I(t) \tag{5}$$

where c varies between 1 and a maximum of d days of infection and I(t) is the total number of infected individuals in the modeled population. In the current model, we consider that there is one infective with Ebola in a given population that fills an airplane, however this number can be higher for more common infectious diseases like influenza. We also assume that the initial number of exposed in the system is zero.

When these i_c^0 infectives come into contact with m_i susceptibles estimated by the pedestrian movement model, the newly infected and the probability of their infection can be estimated using a binomial distribution. In the context of air-travel, the model population is relatively small (a few hundred passengers), hence, contacts are few. We assume that probability of an individual infecting each susceptible is small and number of susceptibles as compared to infected (or exposed) is larger. Under this assumption, we approximated binomial distribution using Poisson distribution. The newly infected at time t and the probability of their infection is as shown in equation (6) below:

$$ I\left(t\right) \sim Poisson\left(\sum_{c=1}^{d}\left(p_c \sum_{i=1}^{i_c^0}\left(\frac{m_i(t-1)s_{r_i}(t-1)}{N} \right)\right)\right) \tag{6} $$

Here, an infective with infectivity p_c placed in a susceptible population would expose $m_i p_c$ members at time t. s_{r_i} represents the number of susceptibles within the radius r_i of infectious individual where infection is possible. The use of Poisson distribution accounts for demographic stochasticity and variations in susceptibility of the population.

The probability-distribution of infection transmission varies depending on the incubation periods and transmission rates for specific diseases and is a primary input data required for the stochastic infection transmission model. For example, for Ebola virus the mean incubation period is 12.7 days [22], with logarithmic increase in virus levels in blood during acute illness phase [23]. The RNA virus copies in the serum is indicative of the transmission probability and we used the corresponding Center for Disease Control and Prevention (CDC) data [23] to obtain the infectivity profile shown in Figure 2. Since, there is no possibility of mortality by infection in the short timescale of the model, we used weighted (by sample size) average of both fatal and nonfatal data from [23] to compute the probabilities in figure 2.

The overall model can be adapted to other directly transmitted infectious diseases as well as other crowded locations (e.g. airport security lines) by modifying the infectivity input and the control parameters in Table 1. Here we used the integrated model to study infection transmission inside an airplane. Inherent uncertainties in human behavior and stochasticity in infection spread make precise prediction of number of infections difficult. Instead, we identify policies and passenger movement strategies that generally lead to reducing the spread of infectious diseases.

TABLE I. Parameters and data ranges used in the computational models.

Parameters	Definition	Estimate/Range	Reference / Notes
$\bar{v}_{0i}$	Walking speed (no obstructions)	1.07 - 1.55 m/s	[18, 21]
γ_i	Random number	0 – 1	[21]
δ	Distance parameter (distance between people in a stationary line)	0.405 m	[21]
ϵ	Repulsive force field parameter	16	[21]
σ	Repulsive force field parameter	0.86 m	[21]

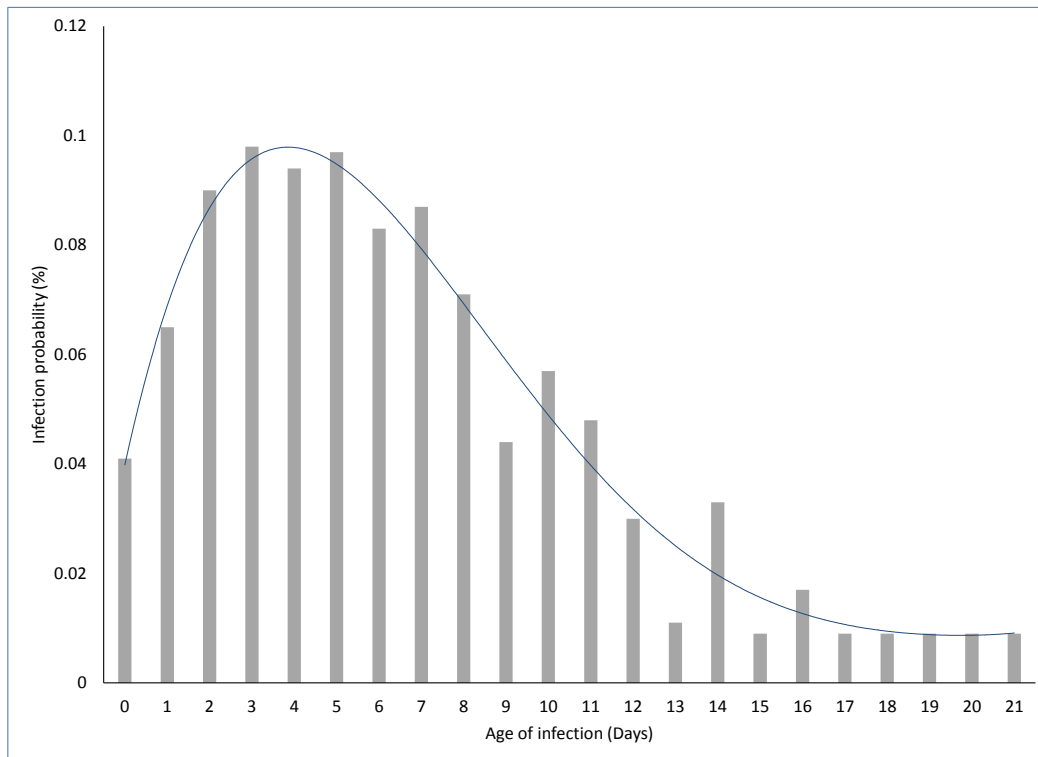| p_c	Infectivity of individual as function of age of infection (c days).	0.01 -0.098	Based on [23] (See Figure 2)
D	Maximum number of days for virus incubation	1-21 days	[23]
i_c^0	Number of infectives with an age of infection of c days	1	Only one infective/ plane assumed

FIG. 2. Distribution of probability of infection vs days since onset of symptoms for Ebola virus; modified and distribution generated using CDC data for RNA copies in serum [23].

III. RESULTS AND DISCUSSION

We consider the situation with one infected individual with Ebola travelling on a commercial airplane. The infective passenger onboard is not identifiable; therefore, we varied the seating position of the infected individual through all the seats in the airplane. At each seating location of the infective, we obtained the mean number of newly infected members and corresponding discrete Poisson distribution using the above formulation. We combined these distributions to evaluate the probability of *k* newly infected passengers when an infected individual is on the airplane at any possible seating position. The mean number of newly infected is the key measure we use in comparing the infection spread using different boarding and deplaning strategies. We used this approach to evaluate air travel policies such as boarding strategies and airplane seating capacity that impact infectious disease spread.

The boarding and exiting strategies have been investigated in earlier studies with respect to minimizing the turn-around time of airplanes at boarding gates [e.g. 19, 20]. Several passenger ingress strategies such

as random, outside-in, back to front, column wise, zone/section style enplanement have been studied. We compare a few of the boarding strategies with respect to spread of infections. In Figure 3, we show that the three-sections boarding method has the highest mean and thus represents the worst strategy for reducing spread of infection. Interestingly, many current airlines use such a strategy with multiple zones or sections. In this method passengers sitting in the front of the aircraft (e.g. first class) board first followed by a middle zone and then the back section of the airplane. Because of this pattern, the passage-way is filled with passengers waiting to get to their seats resulting in clustering and increased exposure with infected passenger and therefore resulting in a higher number of newly infected passengers. The column-wise method, used here, is the same as the outside-inside strategy in a front-to-back manner. This scheme also results in more infected members. For the random and two-sections boarding, passengers close together in a queue may be seated in seats that are wide apart. This leads to arbitrary movement of passengers along the cabin preventing clustering of a group of travelers around the infected passenger which in-turn reduces infection transmission. The two-section and random boarding have the same mean value of two newly infected, although the infection transmission for two-section strategy results in a lower probability of infection at the mean. A two–section strategy involves dividing the plane into two sections and the passengers are randomly boarded within these sections. Our model suggests that this approach may be a good choice to reduce infection transmissions during boarding. We find the similar pattern of results for 144 seat Airbus A320 seating configuration as well as 182 seat Boeing 757-200 seating configuration (see Figure 3 a & b). In these simulations (figures 3, 4 and 5) the airplanes contain a single Ebola infected passenger with infectivity corresponding to one day of infection in an unidentified seating location with a contact radius of 1.2 m.
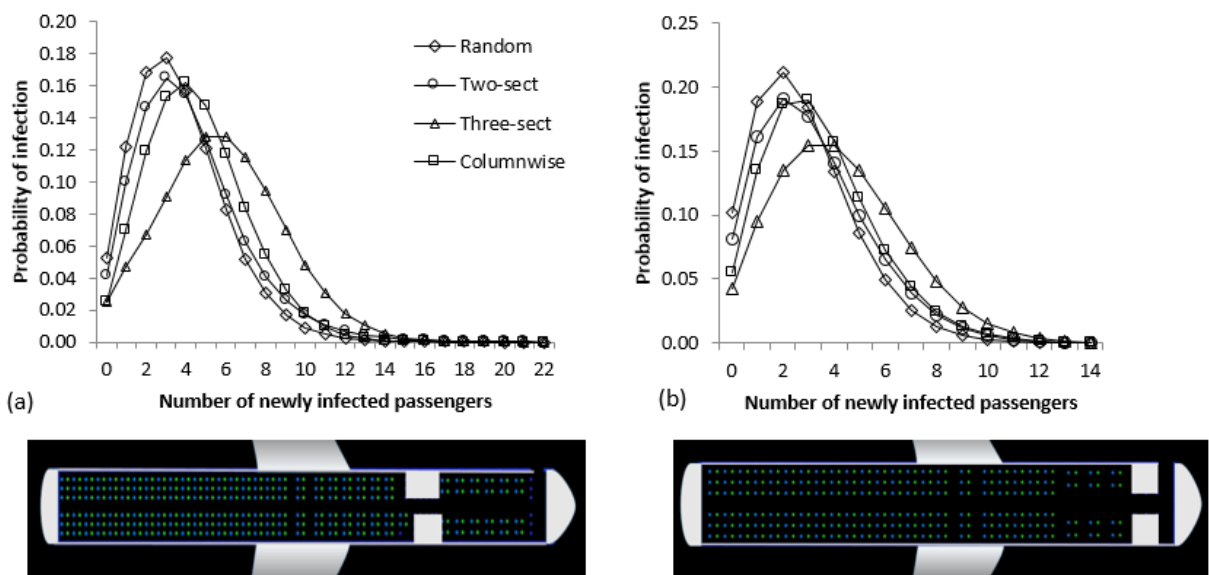

FIG. 3. Infection distribution profile at different boarding strategies for (a) Boeing 757-200 capable of 182 passengers, (b) Airbus A320 capable of 144 passengers. The pictures on the bottom show the corresponding aircraft seating configurations with seats (blue dots) and pedestrians (green dots)

We followed a similar approach for the deplaning strategies. We found that deplaning had a smaller impact on infection dynamics because of the lower number of new contacts and lower time of exposure during the comparatively faster process. In Figure 4, we show a comparison of deplaning strategies for the 182 seat Boeing 757 seating configuration. The different deplaning strategies such as alternating columns, alternating rows, zone wise and baseline (closest to exit - out first) result in similar number of mean infectives. When we compare the probabilities alternate rows and baseline strategies are marginally better. In Figure 5, we compute the mean infectives by combining the egress, ingress, and in-plane movement. It

is apparent that other pedestrian movement strategies can be better than the boarding using multiple zones. We show the worst case situation where an infected individual with peak infectivity is seated at a location that results in the highest number of contacts.
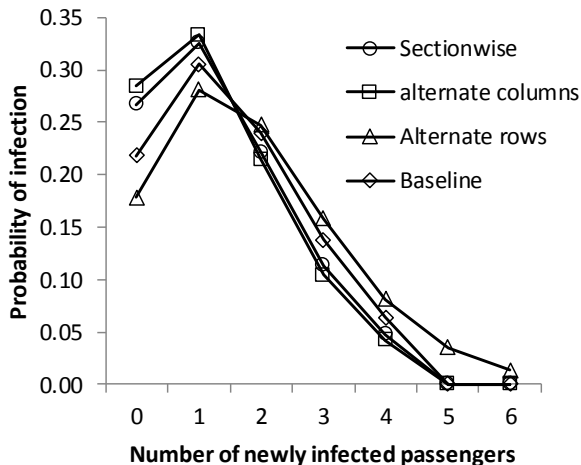

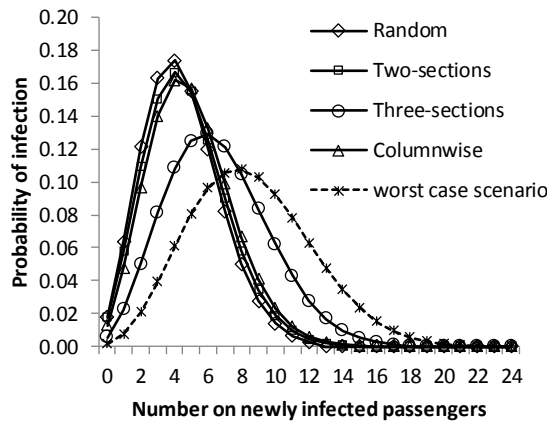FIG. 4. Infection distribution profile for different deplaning strategies for 182 seat Boeing 757

FIG 5. Infection distribution profile for combined baseline egress with different boarding strategies for 182 seat Boeing 757

There is an inherent uncertainty in the human movement behavior as well as the stochasticity in the infection model. Many parameters affect the simulations including airplane size and seating arrangement, the number of infective passengers, the infectivity characterized by days post onset of symptoms, the radius of infection which in turn depends on transmission mechanics (e.g. Coughing, talking etc.), and the susceptibility of population. It is necessary to assign values for some of these parameters for deterministic analysis, however the uncertainty in these parameters needs to be quantified to assess effective air travel policies under a broad set of conditions. We have studied the variations in some of those parameters.

According to the CDC, data a nonfatal Ebola infection lasts for 21 days post onset of symptoms, with highest virus shedding rates and correspondingly highest infectivity in days 3-5 of disease development [23]. The three zone boarding simulations are repeated by varying the number of days of infection for an infective person as we show in Figure 6. The number of mean newly infected passengers clearly varies with the infectivity of the index passenger. During a known outbreak, reported infected passengers will most likely be grounded for further monitoring, but there have been three cases of potentially newly infected passengers travelling through commercial airplanes from the 2014 epidemic [11-13]. A medical professional travelled in two commercial airplanes on October 10th and October 13, 2014 within United States [11]. The index case was tested and confirmed to be infected on October 15th, however it is uncertain if the person was infectious and exhibiting symptoms during the travel dates. Contact tracing indicated no further infections. According to our simulations, the probability of zero new infected cases is about 7% with a fully loaded flight. Note that there were large number of vacant seats in one of the flights which would have increased this probability. We cannot make a direct comparison because it is not known if the index case was infectious [11].

Another critical model parameter is the contact radius which is the minimum distance at which a susceptible passenger in the proximity of the infective can be potentially infected. The distance to which particles travel depends on the particle size and associated fluid mechanics in expiratory events like coughing and talking [24]. Experimental investigations measure particle size in these expiratory events to

be in the range of 0.1 to 10 μm [25, 26, 27]. Droplets emanating from cough of 30 μm and smaller have been estimated to travel over 2 m [24, 27]. The transmission distance also depends on specific disease, for example, SARS has been transmitted by short range droplet based as well as longer range airborne mechanisms [28]. Primary mode of transmission for Ebola is through contact droplets, but studies with monkeys indicate possible transfer through aerosols [29]. Mangili and Gendreau [30] indicate large droplet and airborne mechanisms are possibly highest risk transmission mechanisms during air travel.
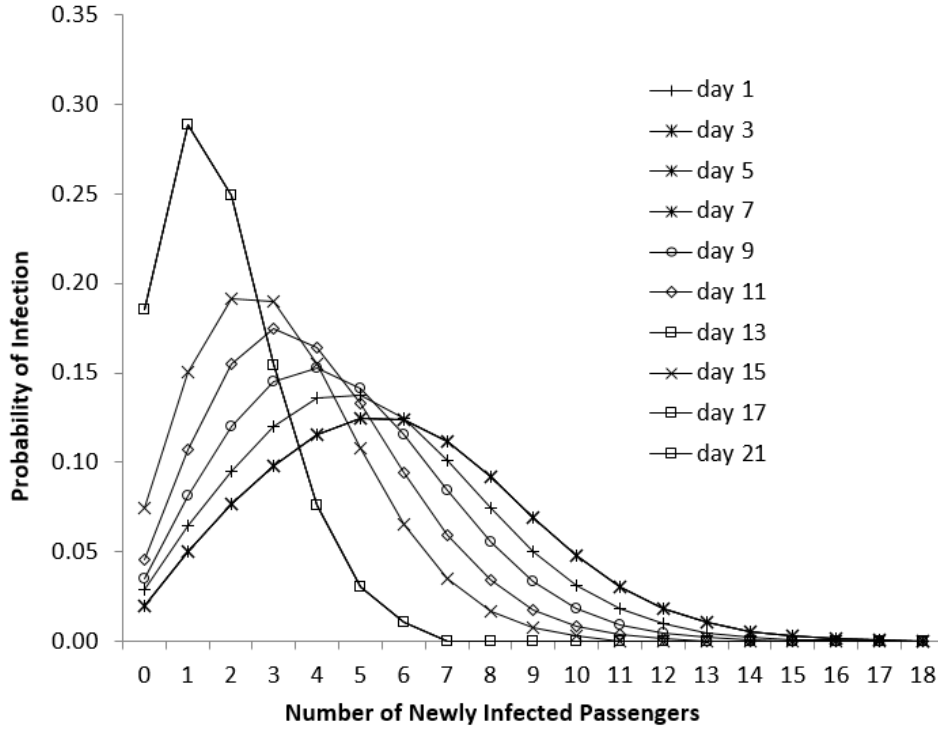

FIG. 6. Infection distribution profile varying the days of infection for index case. Three zone boarding strategy for 182 passenger seating configuration is used for these simulations.
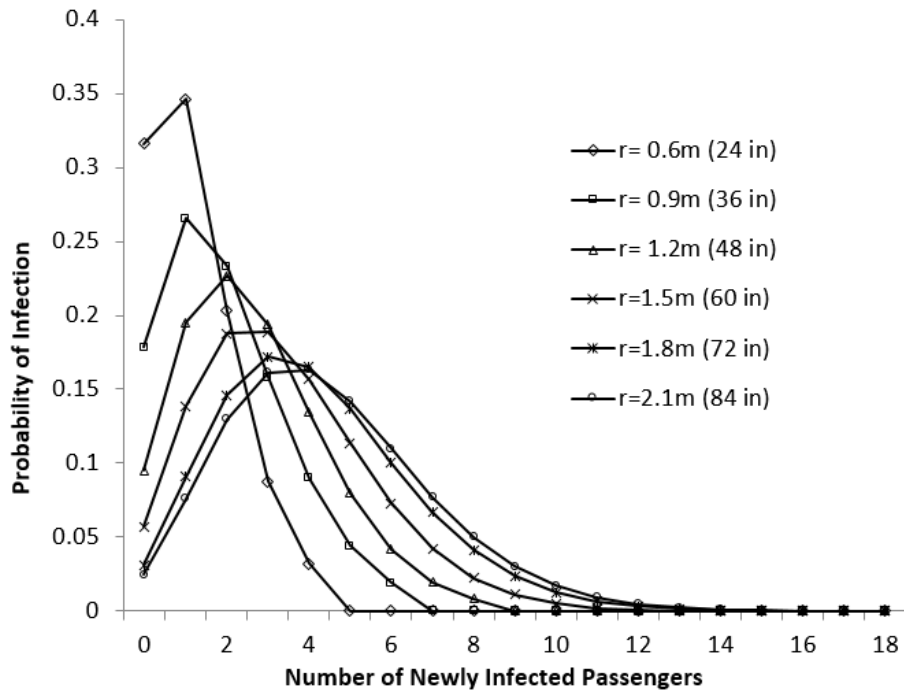
FIG. 7. Infection distribution profile varying the contact radius for infection transmission. Three zone boarding strategy for 182 passenger seating configuration is used for these simulations.
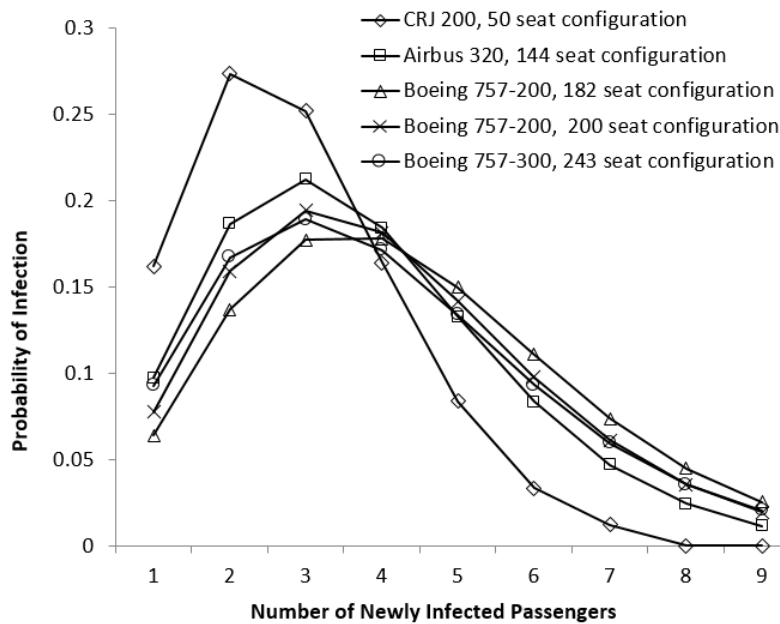

FIG. 8. Infection distribution profile for random boarding strategy varying the airplane size.

We account for the effect of environmental variation and transmission methods on the contact radius by varying it from 0.6 m (24 inch) to 2.1 m (84 inch) as we show in Figure 7. The typical seat width on airplanes is 18 inches (0.45 m). We consider a distance between passenger particles of 24 inches (0.61m)

as a touching distance. The lower end of the range in Figure 7 signifies a contact based and large droplet mechanism while a larger contact radius may be more relevant for aerosol based mechanisms. As expected, the number of newly infected passengers is lower when the contact radius is lower.

Next, we considered the size and the seating capacity of the airplane. In Figure 8, we show the effect of airplane size with a random boarding strategy. Smaller airplanes such as CRJ-200 are better in reducing the spread of infection compared to larger capacity airplanes, however the advantage with smaller seating capacity of airplanes quickly vanishes as the number of seats increase beyond 150. The smaller size of the susceptible population, lower number of susceptibles within a given contact radius and the reduced time of in-plane movement are some of the factors that benefit smaller airplanes.

The improvements obtained for individual flights by these policy changes can benefit substantially over the course of an epidemic. For example, consider the case of 2014 Ebola epidemic: Bogoch *et al.* [14] estimate that without travel restrictions, 41,750 would have used air travel for international destinations in a given month from the highly affected countries of Liberia, Sierra-Leone and Guinea. This is based on data from Sep-Dec 2013. They estimate that under these conditions, without travel restrictions, 7.17 infected travelers per month would travel out bound from these countries. Note that travel restrictions have resulted in very few cases of Ebola infected travelers using commercial airplanes. We aggregate our model results based on the data from [14]. We assume all the passengers traveling are divided equally between A320 and Boeing 757 seating configurations considered in figure 3, and move according to strategies discussed earlier (figures 3, 4 and 5). The mean number of infectives and probability of infection is computed as described earlier and aggregated per month. Our model suggests there is a 67 % probability of generating more than 20 new air-travel related infections per month using the default boarding strategies with these 144 and 182 seat configuration airplanes. This can be reduced to less than 40% by using the better pedestrian movement strategies suggested in figures 3 and 4. In addition, exclusive use of small 50 seater airplanes further reduces the probability of generating 20 infecteds to 13% probability.

IV. SUMMARY

A multiscale model combining social force based pedestrian dynamics and metapopulation stochastic infection dynamics model has been formulated. The model is used to study the dynamics of Ebola virus infection on airplanes specifically during pedestrian movement related to boarding and disembarkation. Specific air travel related policies that potentially mitigate diseases spread are identified. The modeling approach developed here is generic and can be readily modified to other directly transmitted infectious diseases and dense pedestrian spaces.

Acknowledgements

References
1. M. Wilson, Emerging Infectious Diseases 1, 39 (1995).
2. M. R. Moser, T. R. Bender, H. S. Margolis, G. R. Noble, A. P. Kendal and D. G. Ritter, American Journal of Epidemiology 110, 1 (1979).
3. S. J. Olsen, H. L. Chang, T. Y. Cheung, A. F. Tang, T. L. Fisk, S. P. Ooi, H. W. Kuo, D. D. Jiang, K. T. Chen, J. Lando, K. H. Hsu, T.J. Chen and S.F. Dowell, New England Journal of Medicine 349, 2416 (2003).
4. T. A. Kenyon, S. E. Valway, W.W. Ihle, I. M. Onorato and K.G. Castro, New England Journal of Medicine 335, 675 (1996).

5. K. Nelson, K. Marienau, C. Schembri, and S. Redd, Travel Medicine and Infectious Disease 11, 81 (2013).
6. M. A. Widdowson, R. Glass, S. Monroe, R. S. Beard, J. W. Bateman, P. Lurie and C. Johnson, Journal of American Medical Association 293, 1855 (2005).
7. K. Bull, Travel Medicine and Infectious Disease 6, 142 (2008).
8. M. Lipsitch, T. Cohen, B. Cooper, J. M. Robins, S. Ma, L. James, G. Gopalakrishna, S. K. Chew, C. C. Tan, M. H. Samore, D. Fisman and M. Murray, Science 300, 1966 (2003).
9. C. M. Rivers, E. T. Lofgren, M. Marathe, S. Eubank, and B. L. Lewis. arXiv preprint arXiv:1409.4607. (2014)
10. M. J. Keeling and P. Rohani. Modeling infectious diseases in humans and animals. Princeton University Press; 2008.
11. J. J. Regan, R. Jungerman, S. H. Montiel, K. Newsome *et al*. Morbidity and Mortality Weekly Report. 64, 63 (2015).
12. Healthcare worker who tested positive for Ebola flew on Frontier flight day before getting sick. Sky Talk. 2014. http://blogs.star-telegram.com/sky_talk/2014/10/healthcare-worker-who-tested-positive-for-ebola-flew-on-frontier-flight-day-before-getting-sick.html.
13. F. Shuaib, R. Gunnala, E.O. Musa, F.J. Mahoney, O. Oguntimehin, P.M. Nguku, S.B. Nyanti, N. Knight, N. S. Gwarzo, O. Idigbe, A. Nasidi and J.F. Vertefeuille Morbidity and Mortality Weekly Report. 63, 867 (2014).
14. I.I. Bogoch, M. I. Creatore, M. S. Cetron, J. S. Brownstein, N. Pesik, J. Miniota, T. Tam, W. Hu, A. Nicolucci, S. Ahmed, J. W. Yoon, I. Berry, S. I. Hay, A. Anema, A. J. Tatem, D. Macfadden, M. German, and K. Khan, The Lancet 385, 29 (2015).
15. D. Helbing and P. Molnár, Phys. Rev. E 51, 4282 (1995).
16. M.P. Allen, D.J. Tildesley. Computer simulation of liquids. Oxford university press; 1989.
17. R. Knoblauch, M. Pietrucha, and M. Nitzburg, Transportation Research Record: Journal of the Transportation Research Board 1538, 27 (1996).
18. J. Zębala, P. Ciępka and A. Reza, Forensic Science 91, 227, (2012).
19. S. Marelli , G. Mattocks , and R. Merry, Aero Magazine 1, (1998).
20. A. Wald, M. Harmon, and D. Klabjan, Journal of Air Transport Management 36, 101 (2014).
21. S. Namilae, A. Srinivasan, A. Mubayi, M. Scotch, and R. Pahle, Physica A: Statistical Mechanics and Its Applications 465, 248 (2017).
22. M. Eichner, S. F. Dowell, and N. Firese, Osong Public Health and Research Perspectives 2, 3 (2011).
23. Centers for Disease Control and Prevention, Review of human-to-human transmission of Ebola virus, Atlanta, GA: CDC (2014).
24. L. Bourouiba, E. Dehandschoewercker, and J. W. M. Bush, Journal of Fluid Mechanics 745, 537 (2014).
25. L. Morawska, G. Johnson, Z. Ristovski, M. Hargreaves, K. Mengersen, S. Corbett, C. Chao, Y. Li, and D. Katoshevski, Journal of Aerosol Science 40, 256 (2009).
26. R. S. Papineni and F. S. Rosenthal, Journal of Aerosol Medicine 10, 105 (1997).
27. J. K. Gupta, C.H. Lin, and Q. Chen, Indoor Air 19, 517 (2009).
28. R. P. Clark and M. L. D. Calcina-Goff, Journal of the Royal Society Interface 6, (2009).
29. N. Jaax, P. Jahrling, T. Geisbert, J. Geisbert, K. Steele, K. Mckee, D. Nagley, E. Johnson, G. Jaax, and C. Peters, The Lancet 346, 1669 (1995).
30. A. Mangili and M. A. Gendreau. The Lancet 365, 989 (2005).